Missouri University of Science and Technology
Scholars' Mine

International Specialty Conference on Cold-Formed Steel Structures

Wei-Wen Yu International Specialty Conference on Cold-Formed Steel Structures 2016

Nov 9th, 12:00 AM - 12:00 AM

Incorporation of Elastic Local Buckling in a Plain Channel Section Beam Subjected to Double-Curvature Bending: An Effective-Width Approach

Edwin Lim

Barry J. Goodno

James I. Craig

Wei-Wen Yu International Specialty Conference on Cold-Formed Steel Structures
Baltimore, Maryland, U.S.A, November 9 & 10, 2016

Incorporation of Elastic Local Buckling in a Plain Channel Section Beam Subjected to Double-curvature Bending: An Effective-width Approach

Edwin Lim[1], Barry J. Goodno[2], James I. Craig[3]

Abstract

When electrical cabinets are subjected to lateral loads, such as earthquakes, the beams of the cabinet frame typically experience double-curvature bending deformation. These beams are usually constructed from cold-formed plain channel sections so they are vulnerable to elastic local buckling near their ends, where high stresses from applied loads are more likely to develop. To capture local buckling behavior, structural engineers typically use high-fidelity finite element models, but this approach can be complex and computationally expensive. A Timoshenko beam element model is simpler and less computationally costly but it is not capable of capturing local buckling behavior. In this paper, a hybrid Timoshenko beam element model augmented with nonlinear nodal springs is proposed to capture elastic local buckling. Local buckling behavior is computed using cross sectional moment-curvature data generated by an effective-width equation, and the results of computations are validated using a high fidelity finite element model (referred to as the benchmark model) of the beam. The resulting reduced rotational stiffness is incorporated in nonlinear elastic rotational nodal springs introduced at the beam ends. A comparison of the hybrid and benchmark model results is presented to confirm the accuracy of the hybrid model.

[1] PhD Candidate, School of Civil and Environmental Engineering, Georgia Institute of Technology, Atlanta, Georgia, USA
[2] Professor, School of Civil and Environmental Engineering, Georgia Institute of Technology, Atlanta, Georgia, USA
[3] Emeritus Professor, School of Aerospace Engineering, Georgia Institute of Technology, Atlanta, Georgia, USA

Introduction

The frames of electrical cabinets are usually constructed with thin-walled open section cold-formed steel members. Most of these members have a shear center that does not coincide with the sectional centroid, and as a result, any forces applied at the centroid of the cross section will not only deflect but also twist the member. This twisting in an open section will also cause axial deformation (warping) which may or not be restrained at the ends. The complexity of this situation also increases when the limit states of the members, such as elastic local/distortional buckling, are included in an analysis. Localized buckling can develop in these sections because the flanges and the webs are thin. Figure 1 shows the differences between the local and distortional buckling modes for channel sections. For a plain channel section, the local and distortional buckling modes do not significantly differ. However, if additional lips at the end of the flanges are present, the two modes clearly differ.

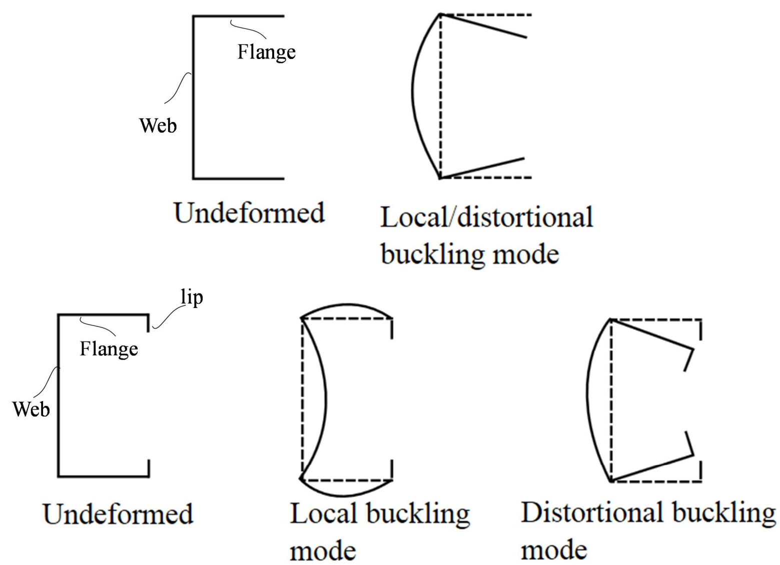

Figure 1 Differences between the local and distortional buckling modes in cold-formed channel section

The post-buckled strength of local and distortional buckling modes is commonly estimated by two general ways: the *effective-width method* and the *direct strength method*. The effective-width method is based on the famous effective-width equation first proposed by Von Karman (Von Karman et al., 1932). Since the first formulation, the equation has undergone several modifications so that it is applicable to the design of relevant structural members. Although the effective-width method is useful for predicting local buckling behavior, it is deficient in predicting distortional buckling behavior. This deficiency is overcome by the application of the finite strip method, which has eventually become the basis for the development of the direct strength method. In the finite strip method, a structural member is divided into a number of longitudinal strips along the member. Each strip has a displacement function which is determined based on the boundary conditions of the member, and the strength of the member is predicted by solving the eigen-buckling equations of the system.

In terms of contemporary structural analysis, the typical practice in modeling the localized buckling behavior of such frame member is to use shell elements in a finite element analysis. This technique may be effective for a very simple beam structure, but the computational complexity and cost increase sharply for more practical cabinet frames. Several researchers have developed a simpler model that captures local buckling behavior. Davies et al. (Davies et al., 1994) and Silvestre et al. (Silvestre and Camotim, 2003) improved a framework called the generalized beam theory (GBT), which has the capability to capture the local and distortional buckling of frame members. However, because of the complexity in formulating the element, it has not been widely applied in commercial structural analysis software.

To model a single member, Wang et al. (Wang and Errera, 1971) developed another model consisting of several rigid beam elements with rotational springs at their ends. The rotational springs represented the moment-rotation relationship of the cross section and had nonlinear properties that were able to capture plasticity in the cross section and local buckling in the member. The ability to capture local buckling behavior was made possible by applying a modification of the effective-width equation proposed by Winter (Winter, 1947) to generate the moment-rotation relationship of the springs. The proposed method, validated by experimental results, exhibited close agreement with the experimental results with an error of less than 10%. Application of this method has also been recently adopted by Ayhan and Schafer (Ayhan and Schafer, 2012). The only difference between the two methods is how the authors developed the moment-rotation relation of the springs. In their approach, Ayhan and Schafer developed an empirical method based on data fitting of the experimental and numerical tests of cold-formed steel members that fail in local and distortional buckling modes and linked the application of this method to ASCE 41 for earthquake analysis. Since the model considers distortional buckling behavior, their method may offer a more general application. Despite the accuracy of this approach, applying the method to a more complex structure is tedious, as the development of a model may require extensive effort.

This general approach can be simplified for application to a cabinet frame structure subjected to a specific type of analysis, such as a pushover analysis commonly employed in seismic design. In such an analysis, the framing members are subjected to double-curvature bending, and in this condition, high stress at the ends of the members is possible and may cause elastic local buckling of the members. In this paper, the elastic local buckling behavior is analyzed using an effective-width method, and the resulting loss in beam rotational stiffness is modeled using, a rotational spring introduced at each end of a beam member, which, in turn, is modeled using simple Timoshenko beam elements commonly found in commercial software. This approach requires less modeling effort than that using the combination of rigid beams and rotational springs. This approach is proposed for application to electrical switchboard cabinets that are subjected to possible elastic local buckling of the framing members.

Elastic Behavior of a Member Subjected to Double-curvature Bending

A cold-formed member constructed from a plain channel section (see Figure 2.a) is considered in this study. In the double-curvature bending condition, the member will initially behave in a linear elastic manner (see Figure 2.b). The end moments of the beam in this state induce a linear stress distribution throughout the web portion of the cross-section, while the flange of the beam is subjected to uniform stress (see Figure 3). The compressive stress in the members will eventually lead to localized buckling as the end moments increase. The moment that causes this behavior is called the “buckling moment” (M_{cr}). After local buckling occurs, the rotational stiffness of the beam ends will decrease (see Figure 2b).

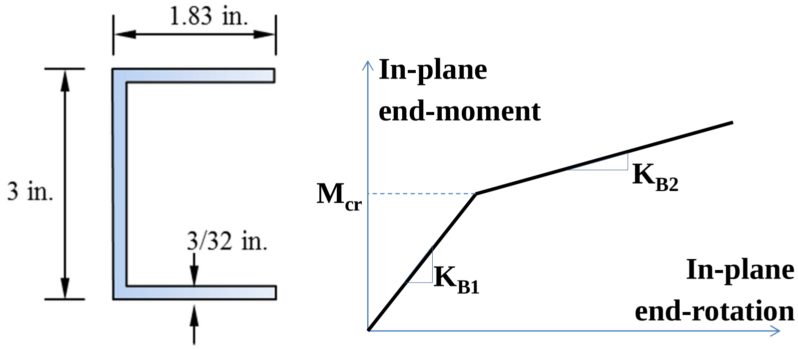

(a) (b)

Figure 2 a) Dimensions of the plain channel section, b) Approximated sketch of the end-moment and end-rotation curve of plain channel member subjected to double-curvature bending

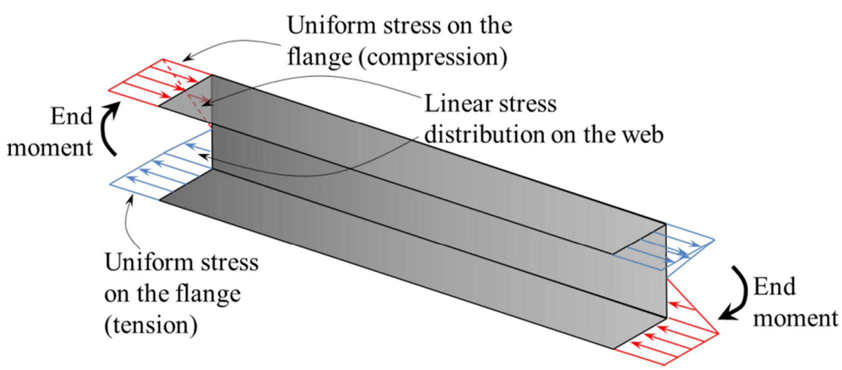

Figure 3 Stress distribution in a channel section member subjected to double-curvature bending

Description of the Hybrid Timoshenko Beam Model

The development of the hybrid model entails the selection of either the Euler-Bernoulli or the Timoshenko beam model, which is commonly found in commercial finite element software. The significant difference between these models is the ability of the Timoshenko model to capture the shear deformation effect in a short member. Because short members may be used in the construction of electrical cabinets, the Timoshenko beam model is selected for the hybrid model. The Timoshenko beam model is able to capture the initial stiffness of the member subjected to double-curvature bending. However, it does not have the capability to capture the local buckling behavior of the member. Therefore, a rotational spring is introduced at each end of the member to capture the stiffness-reducing effect caused by elastic local buckling of the member (see Figure 4a). The rotational springs and the frame elements are arranged in series in direction 3 (in-plane direction), and the property of the springs is typically nonlinear (see Figure 4.b).

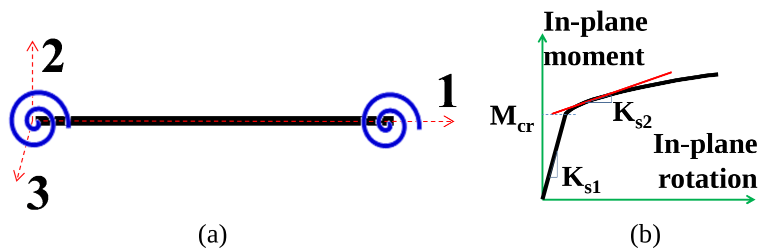

Figure 4 (a) Schematic of the hybrid model, (b) Approximate sketch of the moment-rotation properties of the rotational springs

To identify the properties of the nonlinear springs employed in the hybrid model, a method that is based on the effective-width prediction of the behavior of the beam under double-curvature bending is proposed and investigated. In this method, the end-moment and end-rotation curve of a member subjected to double-curvature bending is calculated using an effective-width approach. Afterward, the properties (stiffness) of the springs can be generated as follows: for a series of connected springs,

$$\frac{1}{K_B} = \frac{1}{K_s} + \frac{1}{K_{TS}} \qquad \text{Equation 1}$$

where

K_B = stiffness of the member subjected to double-curvature bending
K_S = stiffness of the nonlinear spring
K_{TS} = stiffness of the Timoshenko frame model

Thus the required stiffness is given from the following equation

$$K_s = \frac{K_{TS} K_B}{K_{TS} - K_B} \qquad \text{Equation 2}$$

This equation is used to find the initial stiffness (K_{s1}) and the post buckling stiffness (K_{s2}) of the springs shown in Figure 4b. In addition, the intersecting point between linear and nonlinear segments of the moment-rotation curve is determined by the buckling moment obtained from the effective-width prediction of the behavior of the member subjected to double-curvature bending. The method to calculate this behavior is explained in the following section.

Effective-width Prediction of the Behavior of the Plain Channel Beam Subjected to Double-curvature Bending

In the proposed hybrid model, effective-width prediction of the behavior of a plain channel member subjected to double-curvature bending is the basis for generating the properties of the rotational springs used with the finite element model (Timoshenko beam model) of the member. In this prediction, end-rotation of the beam is chosen as the dependent variable, given the known value of the end-moment. Figure 5 shows the general framework used to calculate the end-rotation of the beam. The process is started by collecting the geometrical and material information of a member. Afterward, the buckling moment of the member and the cross-sectional moment-curvature data are calculated. More detailed descriptions of these processes are explained in the following paragraphs. After the cross section moment-curvature data is obtained, the end rotation of the beam is calculated by considering the strain energy of the member contributed by bending and shear deformations of the member. Inclusion of the torsional and warping strain energy may improve the result. However, based on trial calculations, the improvement is insignificant.

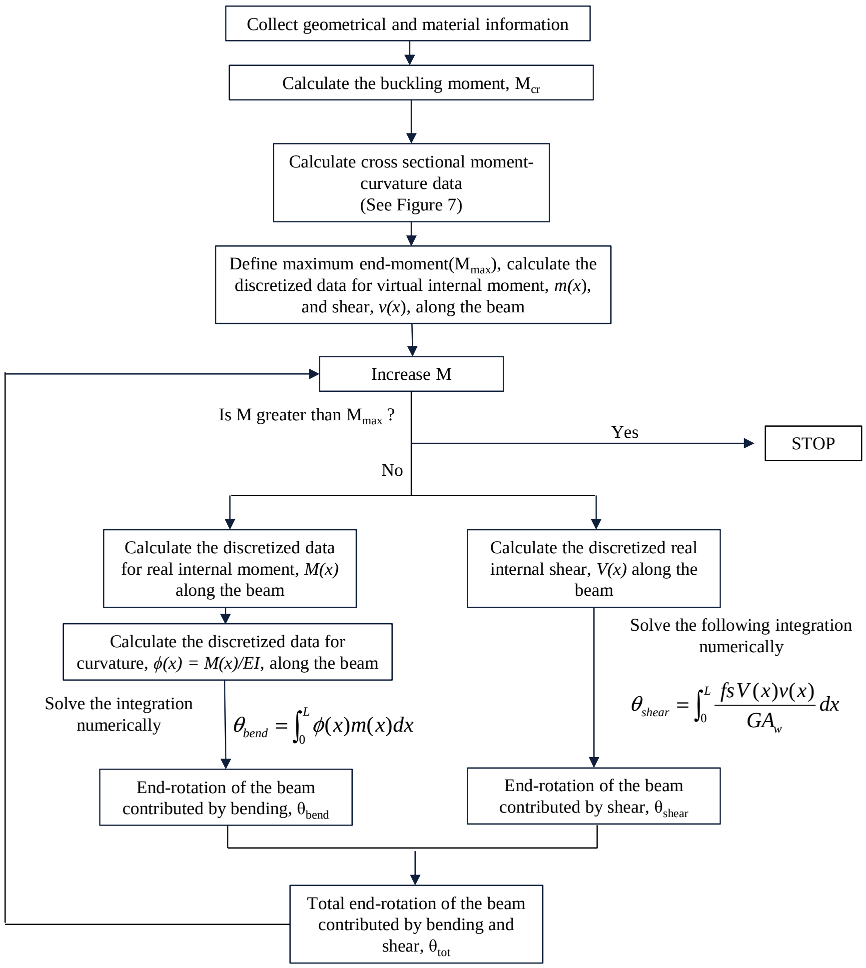

Figure 5 General framework used to calculate the end-rotation of cold-formed member subjected to double-curvature bending

As shown in Figure 5, the calculation of the end rotation of the member requires first the calculation of the buckling moment of the member. The buckling moment is calculated based on buckling stress obtained from a plate model (see Figure 6) subjected to uniformly distributed forces at the transverse edges. These forces represent the compressive forces acting on the flanges of the member.

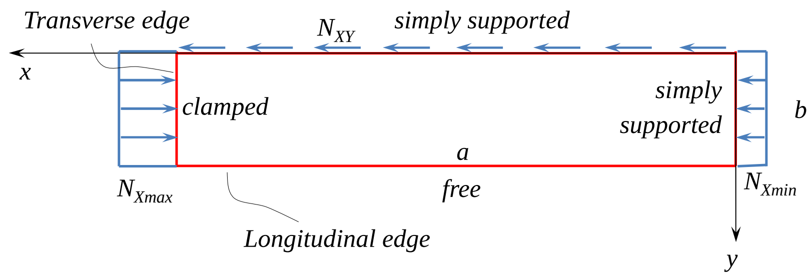

Figure 6 Plate model used to predict the local buckling stress of channel section member

The buckling stress of the plate is then calculated based on the Rayleigh-Ritz approach using the assumed shape function shown in Equation 3.

$$u(x, y) = C_1\left(2\sin\left(\frac{\pi x}{a}\right) + \sin\left(\frac{2\pi x}{a}\right)\right)\left(\sin\left(\frac{\pi y}{2b}\right) + \sinh\left(\frac{\pi y}{2b}\right)\right) \quad \text{Equation 3}$$

where,

u (x,y) = the shape function of the plate model
C_1 = arbitrary constant defined the magnitude of the shape function
a = length of the plate model
b = width of the plate model

Once the buckling stress equation is obtained, it can be used to calculate the buckling moment of the member by: 1) formulating a buckling moment equation of the member based on the buckling stress equation of the plate model using beam theory, and 2) finding the optimum buckling moment from the resulting buckling moment expression.

After the buckling moment and before the end-rotation of the member is obtained, the cross sectional moment-curvature curve is calculated. The slope of this curve is the beam bending rigidity, EI, which is the product of the modulus of elasticity, E, and the second area moment of the section, I (commonly called the moment of inertia). In general, the calculation of the beam rigidity can be divided into two parts: 1) calculation of beam rigidity prior to local buckling, and 2) calculation of beam rigidity after local buckling. Since the modulus of elasticity does not change in both parts, the beam rigidity is sensitive to the change in the sectional second area moment. The sectional second area moment prior to local buckling is based on the original geometry of the cross section. However, the sectional second area moment after local buckling is based on the effective geometry of the cross section. The effective geometry is obtained by reducing the width, b, of the compressed flange using the modified effective width, b_e, given by:

$$b_e = \sqrt{\frac{k_c \pi^2 E t^2}{12\left(1-\mu^2\right)\sigma_{\max}}} \qquad \text{Equation 4}$$

where

b_e = effective width of the element,
k_c = numerical factor obtained from the buckling stress equation of the plate model,
E = Modulus of Elasticity,
μ = Poisson's ratio,
σ_{max} = maximum elastic stress on the element, and
t = thickness of the element.

The modified equation (see Equation 4) is formulated using the general buckling expression under the maximum elastic stress instead of the yield stress of the member as proposed in the original equation by Von Karman. This adjustment is based on the assumption that only elastic local buckling is possible for the framing members of the electrical cabinet due to dynamic loads. Figure 7 on the following page shows the flowchart used to calculate the cross sectional moment-curvature data.

After the cross-sectional moment-curvature data is calculated, the end rotation of the member can be computed following the general framework shown in Figure 5. Once the end-moment and end-rotation of the beam are obtained, the properties of the rotational springs used in the hybrid model can be calculated using Equation 2. All of these processes can also be applied to a member constructed with a plain angle section. However, a slight modification is needed for the plate model used to predict the buckling moment of the member. The plate model shown in Figure 8, which is subjected to linearly varying distributed forces on the transverse edges, is needed. This plate model represents the stress distribution on the web/flange of the member subjected to double-curvature bending.

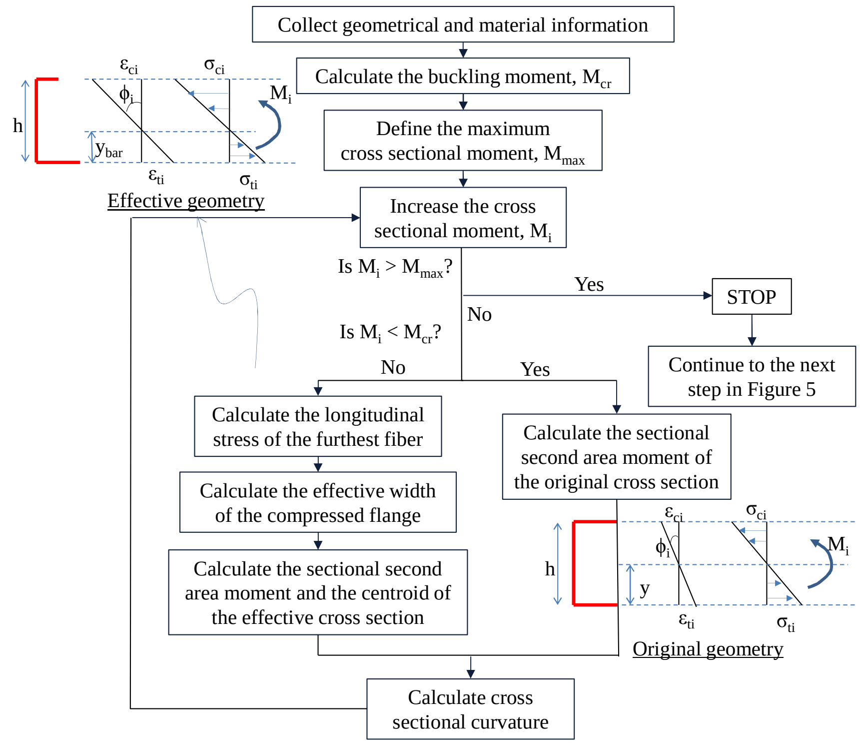

Figure 7 Framework to calculate the cross sectional moment-curvature data

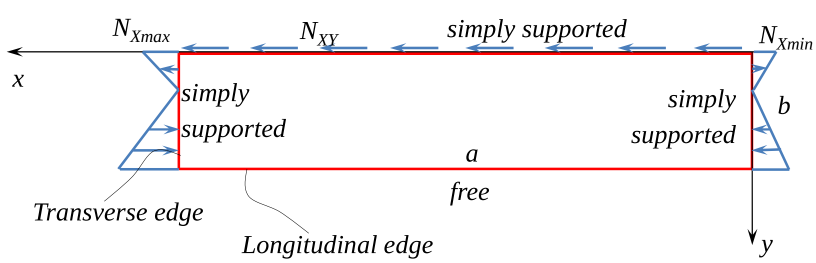

Figure 8 Plate model used to predict the buckling stress of angle section member

For this plate model, the shape function used to calculate the buckling stress is also modified to that shown in the following equation:

$$u(x,y) = C_1\left(\sin\left(\frac{\pi x}{a}\right)\right)\left(\sin\left(\frac{\pi y}{2b}\right) + \sinh\left(\frac{\pi y}{2b}\right)\right) \qquad \text{Equation 5}$$

Note that only the x term of the function is changed. This change is related to the boundary conditions applied to the member to impose the unsymmetric bending condition.

Validation of the Results of the Effective-width Prediction and the Hybrid Model

Validation of the Results of the Effective-width Prediction

The result of the effective-width prediction for a member subjected to double-curvature bending is validated using the result of a finite element model of the member (referred to as the *benchmark model*). The finite element model of the member is developed using shell elements in ABAQUS (ABAQUS, 2012), and the nonlinear geometry effect (2^{nd} order) is included in the analysis, such that it has the capability to capture the elastic local buckling of the member. The model is fixed at both ends and incremental in-plane rotations are applied to those ends to impose double-curvature bending on the member. Two beam specimens representing short (14-in. (0.36-m)) and long (36-in. (0.91-m)) beams are selected to validate the effective-width prediction. The members are constructed from the channel section shown in Figure 2a.

The comparisons between the end-moment and end-rotation of the benchmark model and the effective-width prediction for the beam specimens are presented in Figure 9 on the following page. The results obtained from the analyses of the benchmark model without considering the nonlinear geometry effect (1^{st} order) are also included in the plots to show the stiffness-reducing effect due to the elastic local buckling behavior. Based on these plots, the effective-width framework is able to predict the end-moment and end-rotation of the benchmark models under 2^{nd} order analysis.

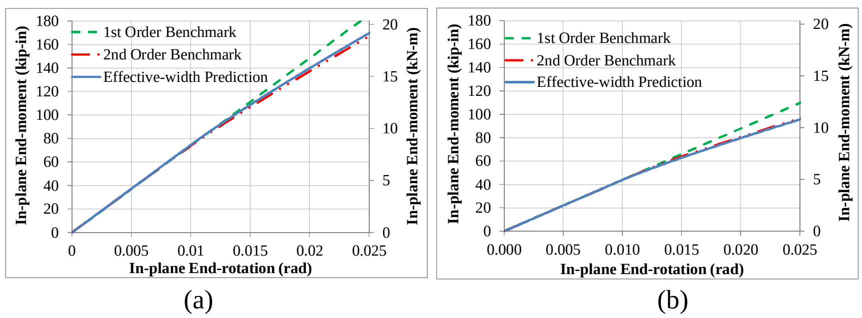

Figure 9 Comparison of the end-moment and end-rotation curve between the effective-width prediction and the benchmark model for the two specimens: (a) 14-in. (0.36-m) length, and (b) 36-in. (0.91-m) length.

In addition to its accuracy, this effective-width framework also offers a possible physical explanation to the growth of distorted region on the beam due to local buckling as the end moments/rotations increase. The distorted region is defined as the portions of the beam over which the curvature no longer has a linear correlation with the moment distribution on the beam. Figure 10 shows the bending moment diagram and the distribution of curvature along the beam for a given end-moment applied to the 36-in.(0.91-m) beam specimen. Note that the bending moment varies linearly along the beam. However, there are some portions of the beam for which the curvature is no longer linear as the end moment is increased. This region will keep growing as the incremental end-rotation/end-moment is increased.

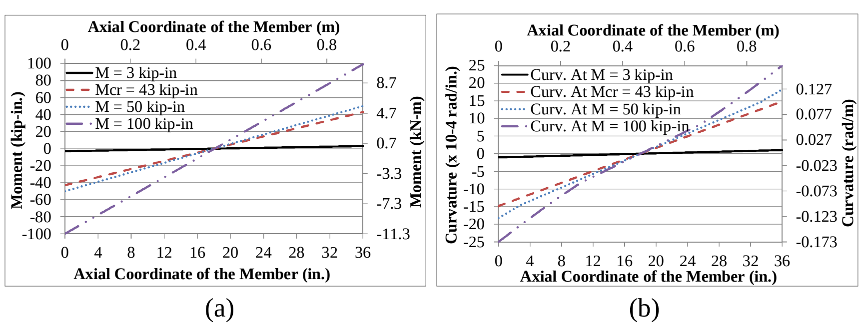

Figure 10 (a) Bending moment diagram and (b) Curvature diagram of the 36-in. (0.91-m)-member in several values of end-moment

Validation of the Results of the Hybrid Model

Next, the effective-width prediction results are used to generate the properties of the rotational end-springs incorporated in the hybrid Timoshenko beam element model. Afterward, this model is analyzed in ABAQUS under double-curvature bending condition. The results of this analysis are then validated to the results of the benchmark model under a similar loading condition. Figure 11 shows the comparisons of the end-moment and end-rotation between the hybrid models and the benchmark models for the 14-in. (0.36 m) and 36-in. (0.91 m) specimens. The hybrid models shows very good agreement with the results obtained from the benchmark models. This result is expected because the properties of the springs are calculated based on an accurate prediction of the behavior of the member.

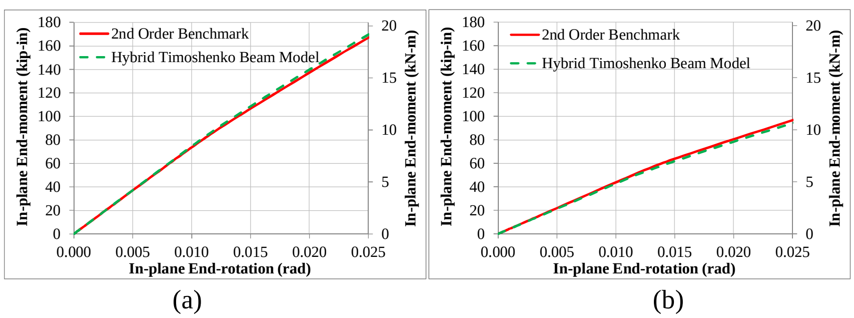

Figure 11 Comparison of the end-moment and the end-rotation curve between the benchmark models and the hybrid Timoshenko beam models for the two specimens: a) 14-in. (0.36 m) length, and b) 36-in. (0.91 m) length.

Conclusions and Future Works

This study proposes a hybrid Timoshenko beam model augmented with a nonlinear rotational spring at each end of a beam member to capture elastic local buckling behavior in the member. The properties of the rotational springs are generated based on the predictions of the behavior of the beam member subjected to double-curvature bending using an effective-width approach. Both the effective-width prediction and the hybrid model are validated to the high fidelity benchmark finite element model of the beam member, and the validations confirm the accuracy of the prediction and the hybrid model. Future work will involve improvement of the hybrid model to handle beam members with a more complex cross section (*e.g.* lipped channel) and to predict the behavior of a cold-formed member under inelastic material condition.

Appendix - References

ABAQUS (2012). ABAQUS/Standard User's Manual, Version 6.12. Providence, RI, ABAQUS.

Ayhan, D. and B. Schafer (2012). Moment-Rotation Characterization of Cold-Formed Steel Beams Depending on Cross-Section Slenderness. Proceedings of the 15th World Conference on Earthquake Engineering.

Bradford, M. A. and M. Azhari (1995). "Buckling of plates with different end conditions using the finite strip method." Computers & structures 56(1): 75-83.

Davies, J., P. Leach and D. Heinz (1994). "Second-order generalised beam theory." Journal of Constructional Steel Research 31(2): 221-241.

Gere, J. M. and B. J. Goodno (2013). Mechanics of materials. Stamford, CT, Cengage Learning.

Silvestre, N. and D. Camotim (2003). "Nonlinear generalized beam theory for cold-formed steel members." International Journal of Structural Stability and Dynamics 3(04): 461-490.

Timoshenko, S. and J. M. Gere (2009). Theory of elastic stability. Mineola, N.Y., Dover Publications.

Timoshenko, S. P. (1945). "Theory of bending, torsion and buckling of thin-walled members of open cross section." Journal of the Franklin Institute 239(4): 249-268.

Timoshenko, S. P. (1945). "Theory of bending, torsion and buckling of thin-walled members of open cross section." Journal of the Franklin Institute 239(3): 201-219.

Von Karman, T., E. E. Sechler and L. Donnell (1932). "The strength of thin plates in compression." Trans. ASME 54(2): 53-57.

Wang, S. and S. Errera (1971). Behavior of cold rolled stainless steel members. International Specialty Conference on Cold-Formed Steel Structures.

Winter, G. (1947). "Strength of thin steel compression flanges." Transactions of the American Society of Civil Engineers 112(1): 527-554.

Yu, W.-W. and R. A. LaBoube (2010). Cold-formed steel design. Hoboken, New Jersey, John Wiley & Sons.

Appendix - Notation

a	= length of plate model
A_w	= cross sectional area of the member contributed to shear deformation effect
b	= width of plate model
E	= modulus of elasticity
f_s	= form factor of the cross sectional area for calculation of end-rotation due to shear deformation effect.
G	= shear modulus
h	= height of the cross section
I	= moment of inertia
K_B	= stiffness of the member
K_{b1}, K_{b2}	= initial and post buckling stiffness of the member
K_s	= stiffness of the rotational spring
K_{s1}, K_{s2}	= initial and post buckling stiffness of the rotational spring
K_{TS}	= stiffness of the Timoshenko beam model
$M(x)$, $m(x)$	= real and virtual internal bending moment, respectively
M_{cr}	= buckling moment of the member
M_i	= incremental moment
M_{max}	= maximum moment
N_{Xmax}, N_{Xmin}, N_{XY}	= maximum, minimum and shear distributed forces applied to the plate model, respectively
$u(x,y)$	= shape function of the plate model
$V(x)$, $v(x)$	= real and virtual internal shear, respectively
y_{bar}	= vertical distance of the centroid of the cross section measured from the bottom fiber of the cross section
ε_{ci}, ε_{ti}	= compressive and tensile strain at the extreme fiber of the cross section subjected to incremental moment i, respectively
$\phi(x)$	= distribution of curvature along the member
σ_{ci}, σ_{ti}	= compressive and tensile stress at the extreme fiber of the cross section subjected to incremental moment i, respectively
θ_{bend}	= in-plane member end-rotation contributed by bending
θ_{shear}	= in-plane member end-rotation contributed by shear
θ_{tot}	= total in-plane member end-rotation contributed by bending and shear